Edelweiss Applied Science and Technology
ISSN: 2576-8484
Vol. 8, No. 6, 4089-4100
2024
Publisher: Learning Gate
DOI: 10.55214/25768484.v8i6.2899

A theoretical study of the output coupler reflectivity effect on the characteristics of Er^{+3} laser pulse at passively q-switching

Zainab Ali Hussein[1*], Abdul- Kareem Mahdi Salih[2]
[1,2]Department of Physics, College of Science, University of Thi-Qar, Thi-Qar, Iraq; zainabalihussein4@gmail.com (Z.A.H.) karimmahdisalih@yahoo.co.uk (A.K.M.S.).

Abstract: The objective of this study deal the effect of the output coupler mirror reflectivity of laser system on behavior and characteristics (duration and energy) of erbium passive Q-switching laser pulse was studied theoretically. In the methods of the study, virtual passive Q-switching laser system consist of major elements such as erbium doped silica as an active medium, Cr+4: YAG crystal used as a saturable absorber, and the mirrors of resonator. Mathematical rate equations model has been used to describe the physical relationship between this element has been solved numerically by Rung - Kutta – Fehlberg method. The results showed regarding the pulse behavior, the increasing value of output coupler mirror reflectivity lead to decreasing of rising and falling time of pulse, so the emission of pulse occur in an advanced time. While regarding the pulse characteristics, the pulse was distinguishable by short duration and high energy, resulting high power of pulse when the output coupler mirror reflectivity increasing. Regarding of results discussion, the study attributes the results to a decrease of the initial and final population inversion density of active medium that results from the increasing value of output coupler mirror reflectivity. Therefore, it is possible to conclude in order to improve the characteristics of erbium passive Q-switching laser pulse; it is appropriate increase the value of output coupler mirror reflectivity within acceptable limits.
Keywords: *Cr+4:YAG, Er +3 doped silica, High power pulses, Laser, Passive Q-switched.*

1. Introduction

Q-switching is excellent technique used in applications which demand high laser intensities. It is mainly applied with solid state lasers in order generation pulses characterized by short duration (10^{-9} - 10^{12}) ^{second} with high power [1,2]. Various applications use this technique extensively, examples include fine material processing, spectroscopy, biomedical treatment, precise distance measurement, and others. [3-5]. There are two types of Q-switching technique, the first type is the active Q-switching, in this type the losses are modulated with an active control element, typically either mechanical, acousto-optic, and electro-optic element [6,7]. The second type is the passive Q-switching technique[8,9]. In this type, an non-linear optical element (saturable absorber material(SA)) added inside the optical cavity[10-12], this element has the characteristic of self-action (passively) without any external action[13,14], it is shows at the initial time high absorption activity of laser photons which are oscillating inside the system cavity, it is an excellent crystal for passive Q-switching in the wavelength range from 800 nm to 1200 nm, because of its good ratio between its ground and excited levels cross-sections, the absorption activity decreases with the time by semi-exponential relationship until reach to the optical bleaching state and allows oscillating photons to transmittance through it [15,16].

In the virtual optical system of this study, the erbium (Er^{+3}) doped silica material has been used as a active medium, Figure 1 illustrates an intra-4f shell transition from its first excited state ($^{4}I_{13/2}$) to the ground state ($^{4}I_{15/2}$) of the Er+3 ion in its trivalent state [17]. Er^{+3} application in optoelectronics has

* Correspondence: zainabalihussein4@gmail.com

caused it to attract a lot of attention,]. While the chromium (Cr^{+4}) doped crystal of YAG has been used as SA material, it is having a great deal of attention as passive Q-switches. The Cr+4 YAG crystals have a wide absorption cross section and a low saturable absorbtion, this results in greater photochemical and thermal stability, and a higher damage threshold [18.19]. Figure 2 shows the energy level of Cr^{+4} [20].

In the present study, we studied the reflectivity of the output coupler mirror effect on the duration, energy, and the power of Er^{+3} passive Q-switching pulse.

(4)

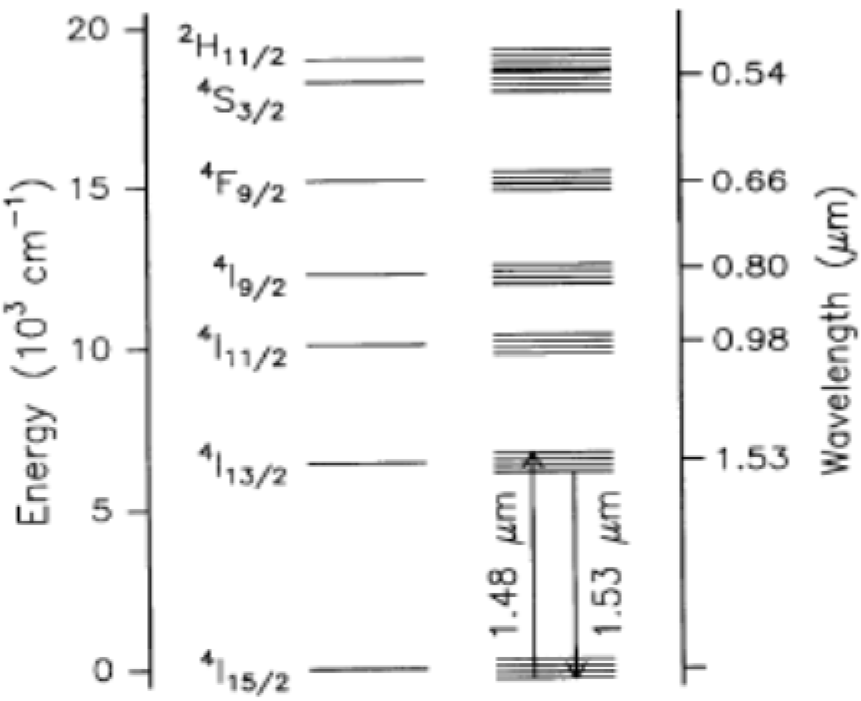

Figure 1.
Energy level diagram of Er+3 [17].

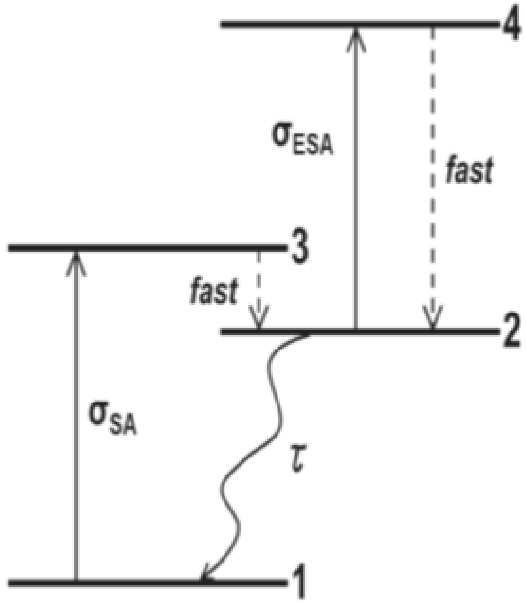

Figure 2.
Energy level diagram of Cr+3 [20].

2. Theory

Coupled rate equations model as the following equations [21] has been used in this study:

$$\frac{d\phi(t)}{dt}=\frac{\phi(t)}{\tau_r}[2\sigma_{am}l_{am}N(t)-2\sigma_{gs}l_{sa}N_{gs}(t)-2\sigma_{es}l_{sa}N_{es}(t)-(\ln(\frac{1}{R_2})+L_{loss})] \quad (1)$$

$$\frac{dN(t)}{dt}=R_p-\gamma c\sigma_{am}\phi(t)N(t)-\frac{N(t)}{\tau_{am}} \quad (2)$$

$$\frac{dn_{gs}(t)}{dt}=\frac{n_{es}(t)}{\tau_{sa}}-2\sigma_{gs}l_{sa}\phi(t)n_{gs}(t)/\tau_r \quad (3)$$

$$\frac{dn_{es}(t)}{dt}=-\frac{n_{es}(t)}{\tau_{sa}}+2\sigma_{gs}l_{sa}\phi(t)n_{gs}(t)/\tau_r \quad (4)$$

Where: ϕ (cm^{-3}) represents the photons number density, $\tau_r=2l_{am}/c$ (s) refer to the transit time for one round –trip, , l_r (cm) is the optical cavity length, σ_{am} (cm^2) is the emission cross section of active medium, c (ms^{-1}) is the speed of light, σ_{gs} (cm^2) is the absorption cross section of SA ground-state, l_{am} (cm) is the AM length, l_{sa} (cm) is the length of SA, n_{gs} (cm^{-3}) represents the ions population of SA ground state, N (cm^{-3}) is the active medium population inversion density, n_{es} (cm^{-3}) represents the ions population of SA exited state, $R_2=(R_1R)^{1/2}$ is the geometric mean of the cavity, R_1 is the total reflectivity of first mirror, R is the output coupler mirror, l_{loss} is the dissipative optical losses for round –trip. σ_{es} (cm^2) is the absorption cross section of SA excited-state, γ is the population reduction factor equal 2, 1 for 3 levels and 4 level of active medium system respectively, R_p is the rate of optical

ISSN: 2576-8484
Vol. 8, No. 6: 4089-4100, 2024
DOI: 10.55214/25768484.v8i6.2899

pumping, τ_{sa} (s) is the lifetime of the excited level of SA, τ_{am} (s) refer to the fluorescence lifetime of the upper laser level. SA has a significantly shorter microseconds lifetime compared to the fluorescence life of the upper laser level [22].

The build-up time for Q-switched laser pulses is typically short, The spontaneous decay in AM and SA can be neglected. The pumping rate is very long compare with the build-up time of Q-switched laser pulses, then can be neglected [23]. then Eq.(2), Eq.(3), and Eq.(4) can be reformulation as the below respectively:

$$\frac{dN(t)}{dt} = -\gamma c \sigma_{am} \phi(t) N(t) \tag{5}$$

$$\frac{dn_{gs}(t)}{dt} = -2\sigma_{gs} l_{sa} \phi(t) n_{gs}(t) / \tau_r \tag{6}$$

$$\frac{dn_{es}(t)}{dt} = 2\sigma_{gs} l_{sa} \phi(t) n_{gs}(t) / \tau_r \tag{7}$$

At the initial time, the photons density number inside the optical cavity is minimum. Also most of SA molecules are in the ground state (n_{gs}), then can be consider $n_{gs} \approx n_{so}$, $n_{es} \approx 0$, where $n_{so} = n_{gs} + n_{es}$ is the total number of SA molecules. Also, at the initial time the SA absorption activity is very high. From Eq.(1) can be consider ($d\phi \ /dt \approx 0$) while cannot consider $\phi(t) = 0$. Then;

$$2\sigma_{am} l_{am} N_o - 2\sigma_{gs} l_{sa} n_{so} - (\ln(\frac{1}{R}) + L_{loss}) = 0 \tag{8}$$

The spatial variation of pulse energy per unit aria (E) at any point in the length of the SA (within the longitudinal direction of the SA) when the pulse passes through the SA can be expressed by [24]:

$$\frac{dE}{dz} = -h\nu n_{so}(1 - \frac{\sigma_{es}}{\sigma_{gs}})[1 - \exp(\frac{-\sigma_{gs} E}{h\nu})] - n_{so}\sigma_{seE} \tag{9}$$

The transmission of SA is known as small-signal transmission or initial transmission (To) at low energy. This situation can be taken into account and consider $\exp(-\frac{\sigma_{gs} E}{h\nu}) \approx (1 - \sigma_{gs} E / h\nu)$, and substituted into Eq. (9) to get:

$$\frac{dE}{dz} = [n_{so}\sigma_{gs} - n_{so}\sigma_{es} - n_{so}\sigma_{es}]E$$

Given that σ_{gs} greater than σ_{es}. the term which include σ_{es} can be neglected, then:

$$\ln E]_{E_{\min}}^{E_{\max}} = n_{so}\sigma_{gs} \int_0^{l_{sa}} dz$$

The optimization of $E_{\max}$ occur when the SA became bleaching to allowed maximum transmission of photons, then can be estimates $E_{\max} \approx \phi_{\max} h\nu$. It is possible to estimate that Emin optimization occurs when the SA has high absorption activity or small signal transmission of photons $E_{\min} \approx T_o \phi_{\max} h\nu$:

$$\ln \frac{E_{\max}}{E_{\min}} = \ln \frac{\phi_{\max} h\nu}{T_o \phi_{\max} h\nu} = \ln(\frac{1}{T_o}) = n_{so}\sigma_{gs} l_{sa}$$

$$T_o = \exp(-n_{so}\sigma_{gs} l_{sa}) \tag{10}$$

$$\ln(\frac{1}{T_o^{\ 2}}) = 2n_{so}\sigma_{gs}l_{sa} \qquad (11)$$

Substituted Eq.(11) into Eq. (8), can be get the initial value of population inversion density as the follow:

$$N_o = \frac{\ln(\frac{1}{T_o^{\ 2}}) + (\ln\frac{1}{R}) + L_{loss}}{2\sigma l_{am}} \qquad (12)$$

At maximum of ϕ , in Eq.(1) can be consider ($\frac{d\phi}{dt} \approx 0$), $n_{es} \approx n_{so}$, or n_{gs} can be neglected.

Threshold population inversion density can be estimated in term of T_o and β, where ($\frac{\sigma_{es}}{\sigma_{gs}} = \beta$) as the following expression:

$$N_{th} = \frac{\beta\ln(\frac{1}{T_o^2}) + \ln(\frac{1}{R}) + L_{loss}}{2\sigma_{am}l_{am}} \qquad (14)$$

3. Results and Discussion

By computer program which prepared in this study, the set of rate equations (1, 5-7) was solved numerically by Rung- Kutta -Fehlberg method. The Table 1 shows the input data which used in computations.

Table 1.
Computations input data.

Parameter	Reference	Parameter	Reference
$l_{am} = 25cm$	[25]	$\sigma_{es} = 2.25\times10^{-19}\,cm^2$	[26]
$l_r = 300cm$		$\sigma_{gs} = 8.75\times10^{-19}\,cm^2$	
$\sigma_{am} = 0.575\times10^{-20}\,cm^2$		$\tau_{sa}\ 4.0\times10^{-6}\,s$	[23]
$\tau_{am} = 5.545\times10^{-3}\,s$		$R2 = 95\%$	[25]
$\gamma = 1$			

Figure 3 represents the time variation of population inversion density (PID)as a function of *R* for three cases of laser passive Q-switching pulses generation.The figure shows that the initial population inversion density (IPID) and final population inversion density (FPID) values decreases as the R value increases. for order verify this behavior for both of IPID and FPID, several cases of several *R* values have been studied as in Figure 4 and Figure 5 , they are shown the decrease in each of IPID and FPID values when *R* increasing and enhanced the Figure 3. The study explains that, the increasing of R value lead to increasing the number of laser photons reflected from the output mirror to the AM, resulting in two important results. The first, the state of accumulation of ions at the excited laser level was prevented by the strong photons' interaction with these ions and forced to move to the lower level and increased stimulated emission, which caused a decrease in the IPID. The second result is a high number of ions discharge from the excited laser level in less time, which caused high decrease in the FPID.

The low value of FPID which is shown in Figure 5 has resulted in the release of a large number of laser photons despite the low IPID value lead to obtained laser pulses characterized by high photons densities as the R value increased as shown in Figure 6. Also observed in Figure 6 is the emission of the pulse occurring in an advanced time as the *R* value increases, It is possible to note that the times at which the pulses in Figure 6 reach their peaks are 550 ns, 516 ns, and 495 ns approximately at *R* = 0.76, 0.84,and 0.94 respectively. To verify this behaviour of pulses which is shown in Figure 6, several cases of several *R* values have been studied as in Figure 7, it is shown the increase in the maximum value of pulse photons when *R* increasing and enhanced the Figure 6. The study explains this du to the decrease in the FPID values Figure 8 shows an increase in the pulse energy with increasing value of *R*. The study explains this because of the increase in the maximum value of the pulse photons, as shown in Figure 6 and 7.

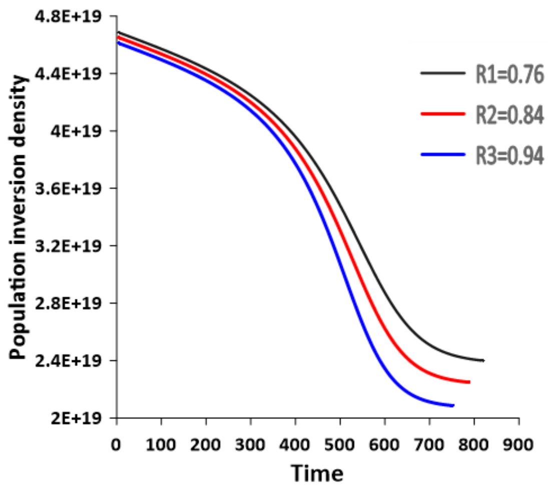

Figure 3.
Profile of population inversion density as a function of time.

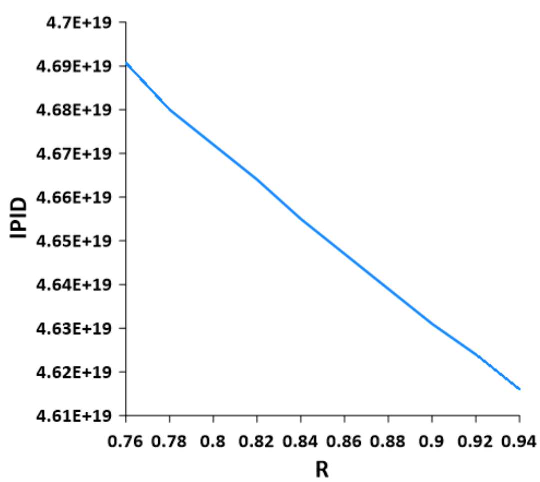

Figure 4.
Initial population inversion density as a function of *R*.

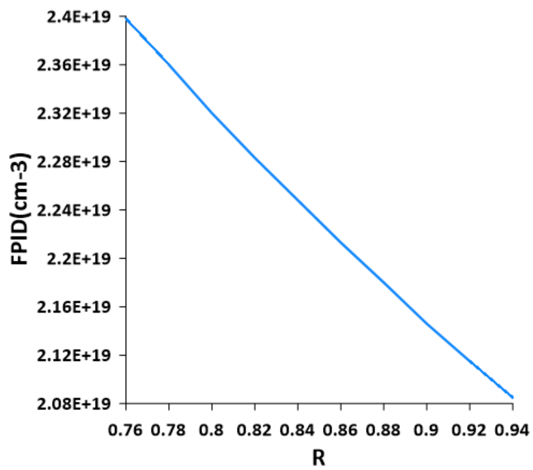

Figure 5.
Final population inversion density as a function of *R*.

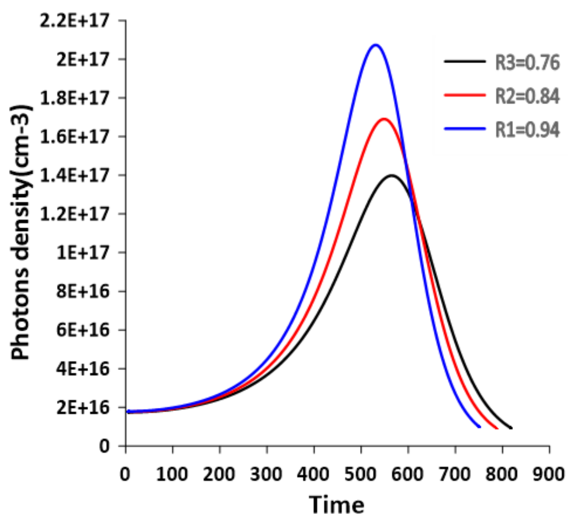

Figure 6.
Photons density of pulses as a function of *R*.

ISSN: 2576-8484
Vol. 8, No. 6: 4089-4100, 2024
DOI: 10.55214/25768484.v8i6.2899

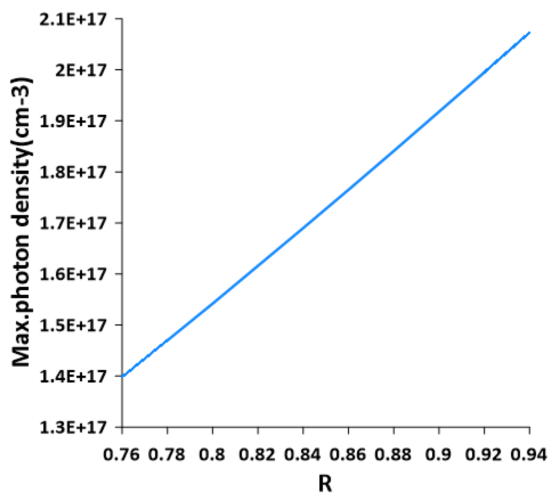

Figure 7.
Maximum photons density as a function of *R*.

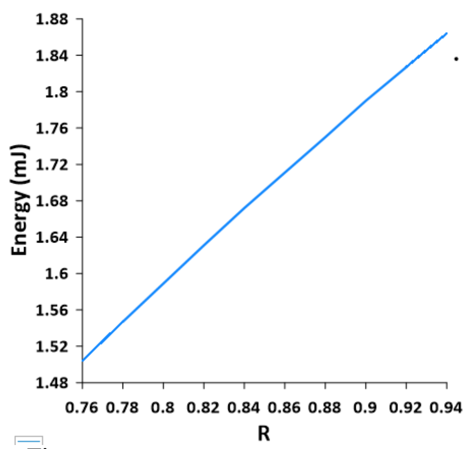

Figure 8.
Pulses energy as a function of *R*.

Figure 9 Represents a decrease in the value of the pulse rising time. The study explains this due to rapid pulse construction by the increase in the photons density with increasing value of *R*.

Figure 10 represents the decrease in the pulse falling time with increasing of *R*, this means that the population inversion density its final value at an earlier time when the value of *R* increases ,and this is reinforced by figure 3. where it is observed The FPID reaches its minimum value at time 828 ns, 796 ns, and 758 ns approximately when *R* =0.76, 0.84,and 0.96 approximately.

ISSN: 2576-8484
Vol. 8, No. 6: 4089-4100, 2024
DOI: 10.55214/25768484.v8i6.2899

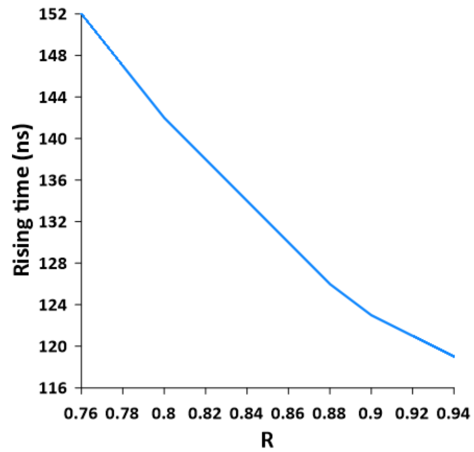

Figure 9.
The rising time of many pulses as a function of R.

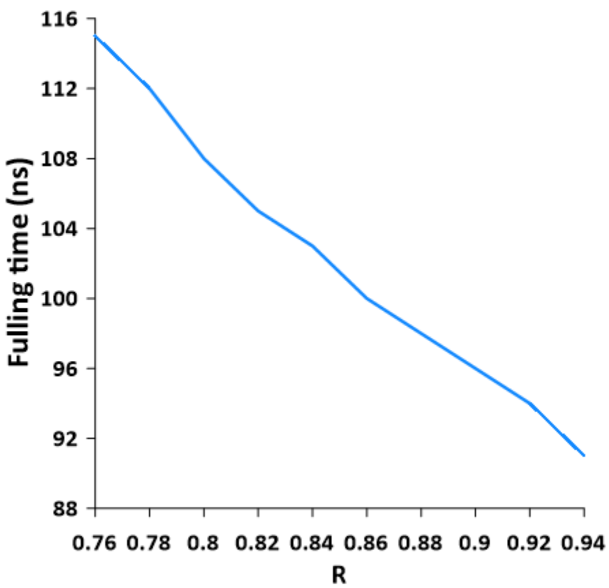

Figure 10.
The fulling time of many pulses as a function of R.

Figure 8. The rising time as a function of R

Figure 11 represents decrease in the value of the pulse duration with an increase in value of *R*. This is due to the decrease in the rising and fulling time values of the pulse as shown in figure (9) and (10), respectively. Figure 11 represents an increase in the pulse power, which is due to the decrease in the duration time as shown in figures (11) and the increasing in energy of pulse as shown in Figure (8).

ISSN: 2576-8484
Vol. 8, No. 6: 4089-4100, 2024
DOI: 10.55214/25768484.v8i6.2899

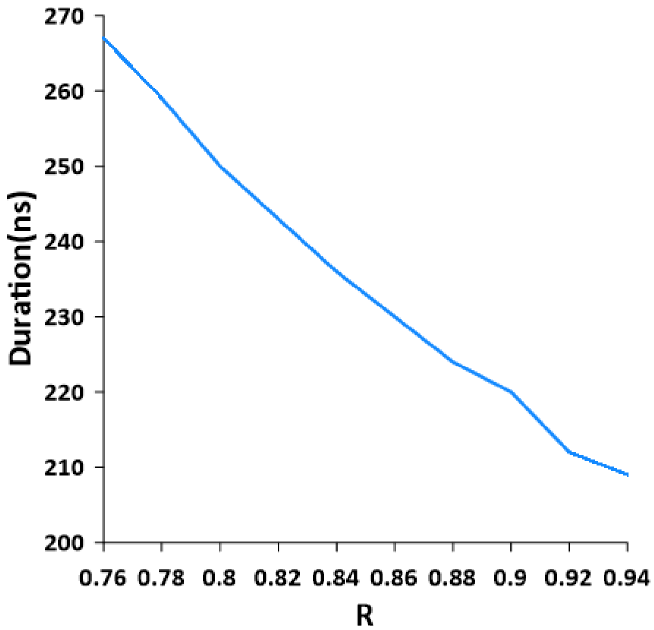

Figure 11.
Duration time of many pulses as a function of R.

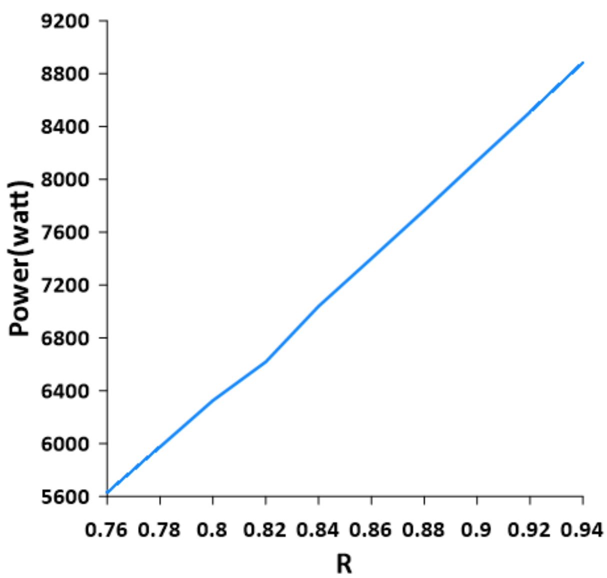

Figure 12.
power of many Pulses as a function of R.

Figure 8. The rising time as a function of R

4. Conclusions

The increasing of the output coupler reflectivity of laser system mirror lead to improve the characteristics of passive Q-switching laser pulses. High photons density have been emitted related to decreasing of final population inversion density with R increasing; caused stimulated emission process has a greater intensity resulting in a high-energy pulse, and the time needed to emit it decreases.

Edelweiss Applied Science and Technology
ISSN: 2576-8484
Vol. 8, No. 6: 4089-4100, 2024
DOI: 10.55214/25768484.v8i6.2899

Improving pulse characteristics was also appearing through short duration resulting in pulse being characterized by high power making it more important in practical applications.

Acknowledgements:
We are deeply appreciative of the provision of essential resources and facilities by University of Thi-Qar, College of Science, Department of Physics, which facilitated the smooth execution of our research activities.

References

[1] S. A. Hussien and A.-K. M. Salih, "Absorption Activity Investigation of Saturable Absorber for Dual Wavelengths in Laser Passive Q-Switching System," *Indian J. Sci. Technol.*, Vol. 17, No. 6, Pp. 577–582, (2024), Doi: 10.17485/ijst/v17i6.2822 .

[2] G. Wang, C. Zhang, H. Jin, L. Xu, and B. Fu, "Self- Q -switching with interferometers," *Phys. Rev. A*, Vol. 109, No. 3, (2024), Doi: 10.1103/PhysRevA.109.033507.

[3] C. Shang, Y.Zhanga, H. Qinc, B. He, C. Zhang, J. Sun, J. Li, J. Ma, X. Ji, L. Xu, and B. Fu, "Review on wavelength-tunable pulsed fiber lasers based on 2D materials," *Opt. Laser Technol.*, Vol. 131, No. September 2019, 2020, (2020), Doi: 10.1016/j.optlastec.106375 .

[4] N.F. Zulkipli, C.Y. Beh ,H.C. Teng, A.R. Muhammad, A.H.A. Rosol, R.A.M. Yu soff , N. Ahmed , S. Omar , M. Yasin, and

[5] S. W.Harun," Neodymium oxide saturable absorber for generating Q-switched and mode-locked pulses in 1.55-micron region," *Optik*Vol. 293, November, (2023), Doi.org/10.1016/j.ijleo.2023.171410.

[6] X. Lei , C. Wieschendorf , L. Hao , J. Firth , L.Silvestri , S. Gross , F. Ladouceur , M. Withford , D. Spence ,and, A. Fuerbach ," Compact actively Q-switched laser for sensing applications,"*Measurement*,Vol.173, March (2021), Doi.org/10.1016/j.measurement.2020.108631 C. Sun," High energy and high frequency electro-optic Q-switching laser with alternating output of energy amplitude,"*Optik*,Volume 200, January,(2020), Doi.org/10.1016/j.ijleo.2019.163287 .

[7] E. E Popov, A .A Sergeev, A. P Pogoda, V. M Petrov and A. S Boreysho," Electro–optic Q-switched Cr:LiSAF laser," *Journal of Physics Conference Series*, November, (2021),DOI:10.1088/1742-6596/2094/2/022034.

[8] J. Tang, Z. Bai, D. Zhang, Y. Qi, J. Ding, Y. Wang, and Z. Lu, "Advances in All- Solid-State Passively Q-Switched Lasers Based on Cr^{4+}:YAG Saturable Absorber," *Photonics* , *8*(4), 93; (2021), Doi.org/10.3390/photonics8040093 .

[9] X.L.Wang, X.J.Wang, J.Dong," Sub-nanosecond, high peak power Yb: YAG/Cr^{4+}: YAG/YVO_4 passively Q-switched Raman micro-laser operating at 1134 nm," *J. Lumin.* , 234 , (2021), Doi.org/10.1016/j.jlumin.2021.117955.

[10] T. Erneux and G. Kozyreff, "Analytical theory of gain-switched laser pulses: From Lotka-Volterra slow-fast dynamics to passive Q switching," *Phys. Rev. E*, Vol. 106, No. 2, Pp. 1–11, (2022), Doi: 10.1103/PhysRevE.106.024205.

[11] B. Nizamani, B. Nizamania, A.A.A. Jafryb, M.I.M. Abdul Khudusc, F.A. Memond, A. Shuhaimie, N. Kasimb, E. Hanafia, M. Yasinf, and S.W. Haruna, "Indium tin oxide coated D-shape fiber as saturable absorber for passively Q-switched erbium-doped fiber laser," *Opt. Laser Technol.*, Vol. 124, No. December 2019, (2020), Doi: 10.1016/j.optlastec.2019.105998.

[12] S, Austin, "Construction and Passive Q-Switching of a Ring-Cavity Erbium- Doped Fiber Laser Using Carbon Nanotubes as a Saturable Absorber", *Graduate Theses - Physics and Optical Engineering*, (2017).

[13] C.A. Brandus, M. Greculeasa, A. Broasca, F. Voicu, L. Gheorghe, and N. Pavel," Diode-pumped bifunctional Nd:LGSB laser passively Q-switched by a Cr^{4+}:YAG saturable absorber, *Optical Materials Express*, Vol. 11, Issue 3, Pp. 685-694, (2021), Doi.org/10.1364/OME.416425.

[14] Y.Fan , C. Zah, D. Wu, C. Gao, Y. Li, Xi. Liu, "Diode pumped passively Q- switched Nd:YAG/Cr:YAG solid-state lasers with a stable output of millijoules at 1064 nm over a wide temperature range," *Proc. of SPIE* ,Vol. 11261 112610N-1, (2020), Doi: 10.1117/12.2543934.

[15] A. A.Salman," Multiwavelength Q-switched Doped Fiber Laser Based on Nanoparticle Saturable Absorbers," A Thesis, *University of Baghdad, Institute of Laser for Postgraduate Studies*, (2019).

[16] A. M. Salih," Numerical analysis of molecules intersystem crossingeffect on a passively Q-switched laser pulse characteristics," *Iraqi Journal of Physics*, Vol. 10, Issue 17 ,30 Jun,(2012).

[17] A. Polman, "Erbium as a probe of everything, " *Phys. B Condens. Matter*, 300. 78–90, (2001).

[18] X. Wang, C. Zhang, Y. Zhang, S. Fan, X. Ma, and W. Cheng, "Sub-Nanosecond, High Peak Power Yb:YAG/Cr4+:YAG/YVO4 Passively Q-Switched Raman Microchip Laser with the Emission of Multiple Pulses," *Photonics*, Vol. 11, No. 1, (2024), Doi: 10.3390/photonics11010061 .

[19] M. E. Jazi and M. Soltanolkotabi, "Investigation of EffectivParameters on Pulsed Nd : YAG Passive Q-Switched Laser," *International Journal of Optics and Photonics (IJOP)*, vol. 5, no. 1, (2011).

[20] M. Tsunekane and T. Taira, "Direct measurement of temporal transmission distribution of a saturable absorber in a passively Q- switched laser," *IEEE J. Quantum Electron.*, Vol. 52, No. 5, (2016), Doi: 10.1109/JQE.2016.2541922.

[21] Z. Ali, Z. Abdulsada, N. Arasavalli, S. Kadhim, and H. Akram, "Initial Transmission Influence on Saturable Absorber Absorption Activity of Passive Q-Switching Erbium -Doped Fiber Laser System," *Univ. Thi-Qar J. Sci.*, Vol. 10, No. 2, Pp. 224–229, (2023), Doi: 10.32792/utq/utjsci/v10i2.1139 .

[22] D. S. Hussein and A. M. Salih, "Simulation of fiber length effect on the pulse characteristics of passively Q-switching Yb +3 doped fiber laser," *Test engineering & management*, 83 22233– 22240, (2020).

[23] M. A. Belov, L. I. Burov, and L. G. Krylova, "Influence of the Cr4+: YAG saturable absorber parameters on output characteristics of the Nd3+: LSB laser Q- switched regime," *Nonlinear Phenom. Complex Syst.*, Vol. 18, No. 2, Pp. 140–148, (2015).

[24] A. S. Majli and A. M. Salih, "Simulation of active medium emission cross section influence on passive q-switching laser pulse characteristics,"*NeuroQuantology*, Vol. 18, No. 5, (2020), Doi: .14704/nq.2020.18.5.NQ20169 .

[25] D. Savastru, S. Miclos, and I. Lancranjan, "Theoretical Analysis of a passively Q-Switched Erbium Doped Fiber Laser," *Romanian Association of Nonconventional Technologies*, 147–53, (2).

[26] D.Savastru, R. Savastru,S. Miclos,and I. Lancranjan," Numerical Analysis of Passively Q-Switched Er and Yb Doped Fiber Laser," *Piers Proceeding, Stockholm, Sweden*, 12, (2013).